Supplementary materials

Supplementary materials (SM) to the manuscript 'Squeezed waveguides as a framework to study vowel-like acoustic resonances' present a comprehensive overview of used literature on vowel formants and area functions, additional theoretical results for the SWVT framework and details of its experimental validation.

1 Illustration of pertinent literature values

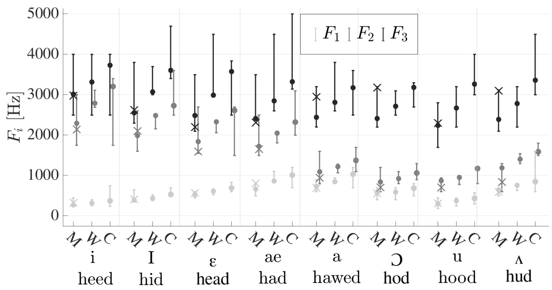

(a) vowel formants: F_1, F_2, F_3

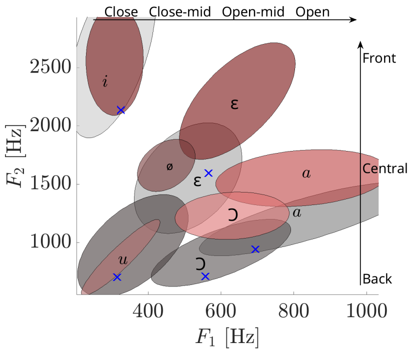

(b) vowel formant space (F_1, F_2)

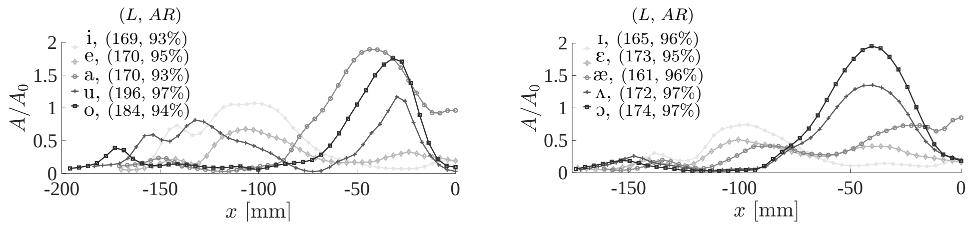

(c) vowel area functions $A(x)$

Figure 1: Literature values for American English speakers (43 adult men (M), 53 adult woman (W), 43 children (C)) and for French speakers (10 adult men (M), 9 adult woman (W)): a) mean (•) and frequency range (bars) of vowel formants F_1, F_2 and F_3 (in Hz) in American English speakers and values (×, adult male) from Story, 2008; b) formant space (F_1, F_2) for American English (gray) and French (red) vowels, showing thumb rules of the influence of area reduction (on F_1) and its location (on F_2). Reference formants (×) for an adult American English speaker (Story, 2008); c) MRI-based vowel area functions $A(x)$ (labelled MRI_0) normalized by $A_0 = 490$ mm^2 for an adult male American English speaker associated with reference formants; VT length L (in mm) and VT area reduction $AR = \min(A(x))/A_0$ (in %).

2 SWVT framework

2.1 SWVT framework: MRI_I and MRI_{II} tailored area functions from MRI_0

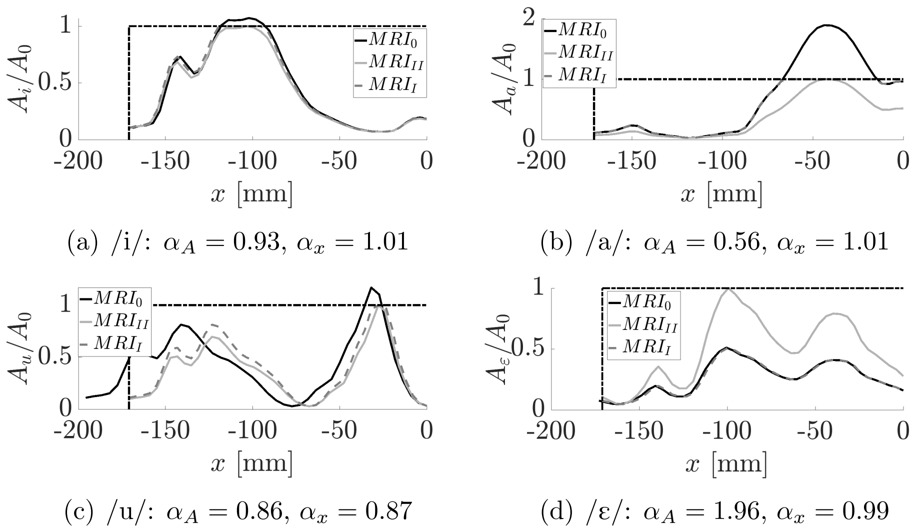

Figure 2: Normalized MRI-based – MRI_0 (black full line), MRI_I (dashed line), MRI_{II} (light gray full line) – area functions $A_{\text{vowel}}(x)/A_0$ for the vowels /i/, /a/, /u/ and /ɛ/,. The SWVT domain boundary, defined by $A(x) = A_0$ over the interval $-L_0 \leq x \leq 0$, is shown as a dash-dot line. Scaling factors α_A and α_x are given.

2.2 SWVT framework: SWVT parameter selection w.r.t. theoretical resonance invariants from MRI_{II}

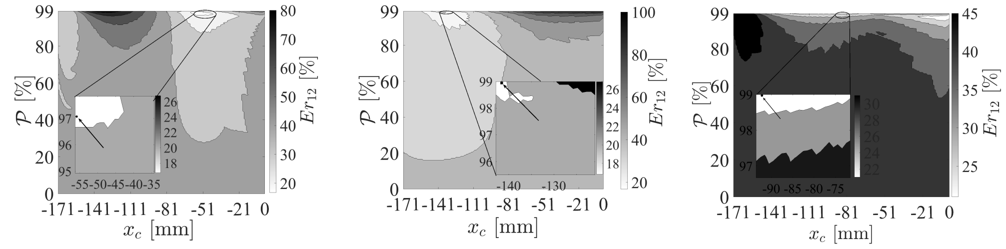

(a) /i/: (23,-52,98)) (b) /a/: (17,-142,99) (c) /u/: (21,-94,99)

Figure 3: Relative differences Er_{12} for theoretical resonances of SWVT parameter subset ($L_0 = 180$ mm$, l_c = 0$ mm$, x_c, \mathcal{P}$) with respect to vowel formants (F_1, F_2) (Story) for /i/, /a/ and /u/. Minimum differences $\min(Er_{12})$ (in %) and corresponding x_c (in mm) and $\mathcal{P}$ (in %) are indicated between brackets (see arrow in zoom).

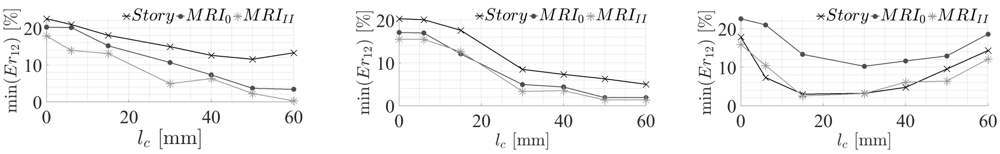

(a) /i/ (b) /a/ (c) /u/

Figure 4: Minima of relative differences Er_{12} for $l_c \leq 60$ mm for theoretical resonances of SWVT parameter subset ($L_0 = 180$ mm$, l_c, x_c, \mathcal{P}$) with respect to vowel formants (F_1, F_2) (Story), theoretical resonances from area functions MRI_0 (MRI_0) and resonance invariants from MRI_{II} (MRI_{II}) for vowels /i/, /u/ and /a/.

2.3 SWVT framework: SWVT area function selection for vowels /i/, /a/ and /u/

2.3.1 One constriction: SWVT selections in $(L_0 = 180\ \mathbf{mm}, l_c = 0\ \mathbf{mm}, x_c, \mathcal{P})$

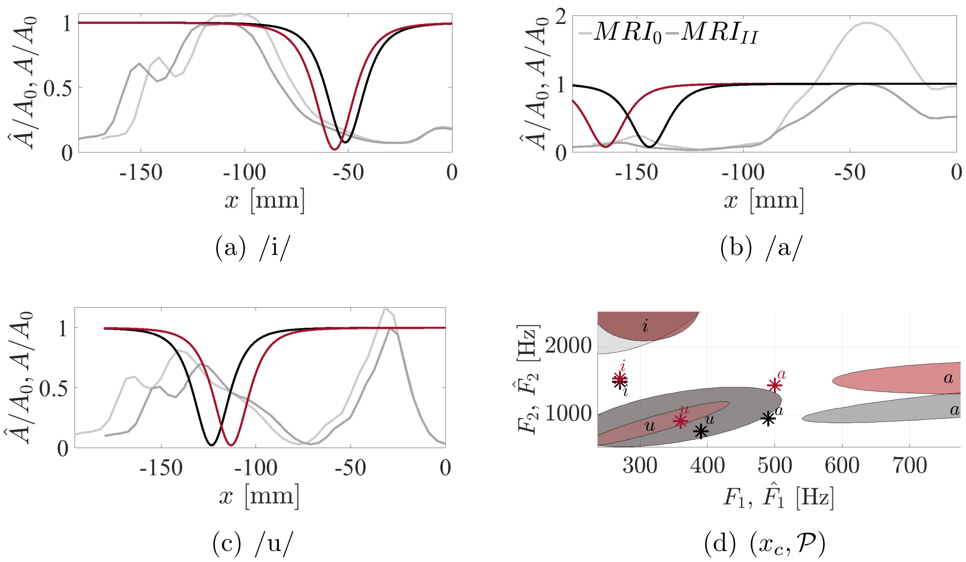

Figure 5: Selected SWVT area functions $\hat{A}(x)$ normalized by $A_0 = 490\ \mathrm{mm}^2$ and corresponding theoretical resonances $(\hat{F}_1, \hat{F}_2)$ for the parameter subset $(L_0 = 180\ \mathrm{mm}, l_c = 0\ \mathrm{mm}, x_c, \mathcal{P})$ for American English (black) and French (red) vowels /i/, /a/, and /u/. As a reference, VT area functions $A(x)$ (MRI_0 in light gray) and reshaped area functions (MRI_{II} in dark gray) are plotted.

2.3.2 One constriction: SWVT selections in $(L_0 = 180\ \mathbf{mm}, l_c, x_c, \mathcal{P})$

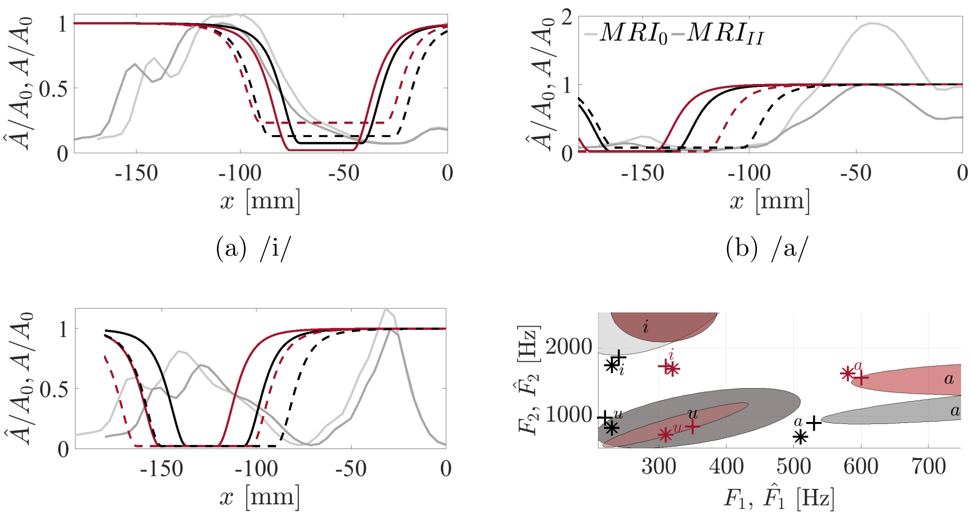

(a) /i/ (b) /a/ (c) /u/ (d) $(\hat{F}_1, \hat{F}_2)$.

Figure 6: Selected SWVT area functions $\hat{A}(x)$ normalized by $A_0 = 490\ \text{mm}^2$ and corresponding theoretical resonances $(\hat{F}_1, \hat{F}_2)$ for the parameter subset $(L_0 = 180\ \text{mm}, l_c \in \{30, 60\}\ \text{mm}, x_c, \mathcal{P})$ with $l_c = 30$ mm (full line, $+$) and $l_c = 60$ mm (dashed line, $*$) for American English (black) and French (red) vowels /i/, /a/, and /u/. As a reference, VT area functions $A(x)$ (MRI_0 in light gray) and reshaped area functions (MRI_{II} in dark gray) are plotted.

2.3.3 Two constrictions: SWVT selections in $(L_0 = 180$ mm$, l_{c,1} = 0$ mm$, x_{c,1}, \mathcal{P}_1, l_{c,2} = 0$ mm$, x_{c,2}, \mathcal{P}_2)$

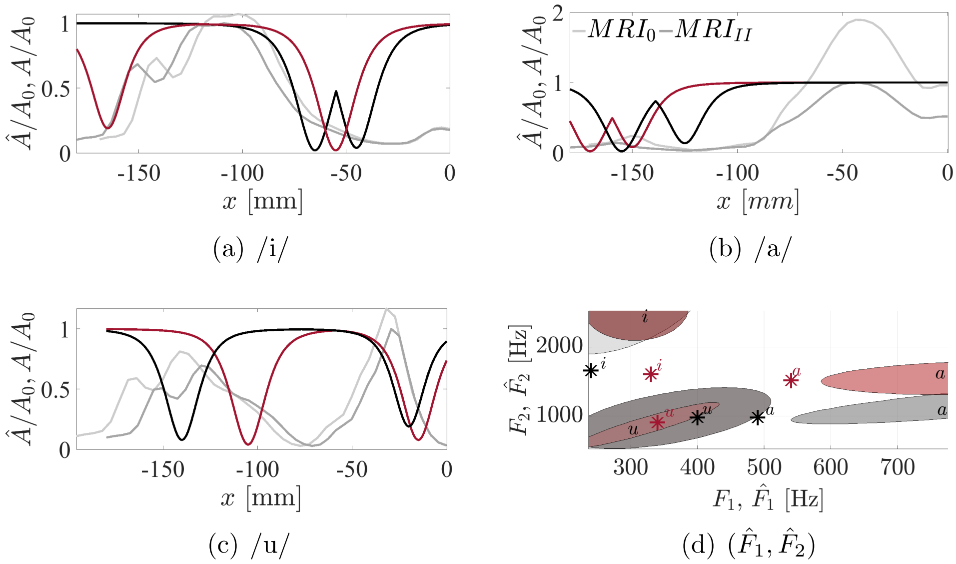

Figure 7: Selected SWVT area functions $\hat{A}(x)$ normalized by $A_0 = 490$ mm^2 and corresponding theoretical resonances $(\hat{F}_1, \hat{F}_2)$ for the parameter subset $(L_0 = 180$ mm$, l_{c,1} = 0$ mm$, x_{c,1}, \mathcal{P}_1, l_{c,2} = 0$ mm$, x_{c,2}, \mathcal{P}_2)$ for American English (black) and French (red) vowels /i/, /a/, and /u/. As a reference, VT area functions $A(x)$ (MRI_0 in light gray) and reshaped area functions (MRI_{II} in dark gray) are plotted.

2.3.4 Two constrictions: SWVT selections in $(L_0 = 180 \text{ mm}, l_{c,1}, x_{c,1}, \mathcal{P}_1, l_{c,2}, x_{c,2}, \mathcal{P}_2)$

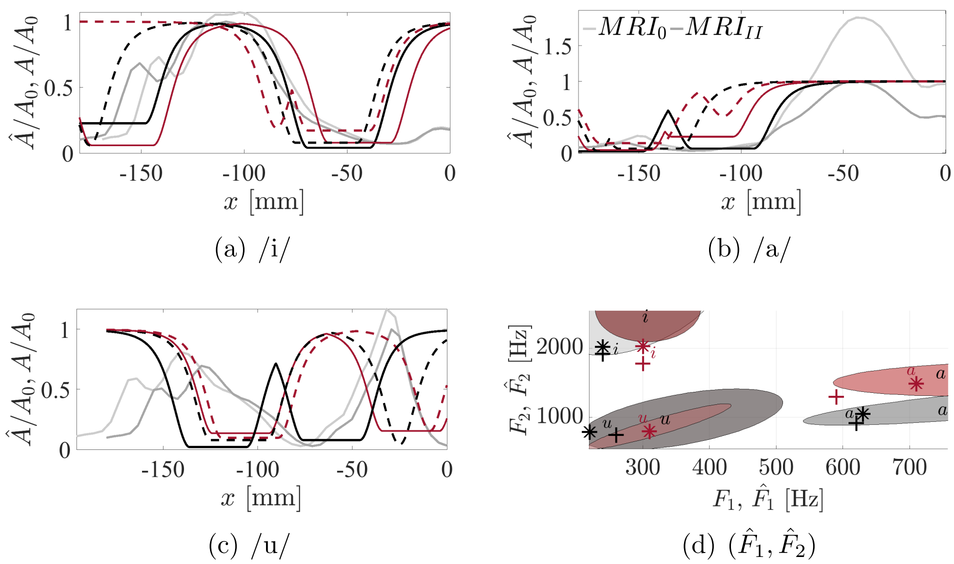

Figure 8: Selected SWVT area functions $\hat{A}(x)$ normalized by $A_0 = 490$ mm^2 and corresponding theoretical resonances $(\hat{F}_1, \hat{F}_2)$ for the parameter subset $(L_0 = 180 \text{ mm}, l_{c,1}, x_{c,1}, \mathcal{P}_1, l_{c,2}, x_{c,2}, \mathcal{P}_2)$ with $l_{c,1} = l_{c,2} = 30$ mm (full line, $*$), $l_{c,1}, l_{c,2} \in \{0, 30\}$ mm with $l_{c,1} \neq l_{c,2}$ (dashed line, $+$) for American English (black) and French (red) vowels /i/, /a/, and /u/. As a reference, VT area functions $A(x)$ (MRI_0 in light gray) and reshaped area functions (MRI_{II} in dark gray) are plotted.

3 Experimental validation

3.1 Experimental validation: experimental waveguides, rigid (R) and molded (M)

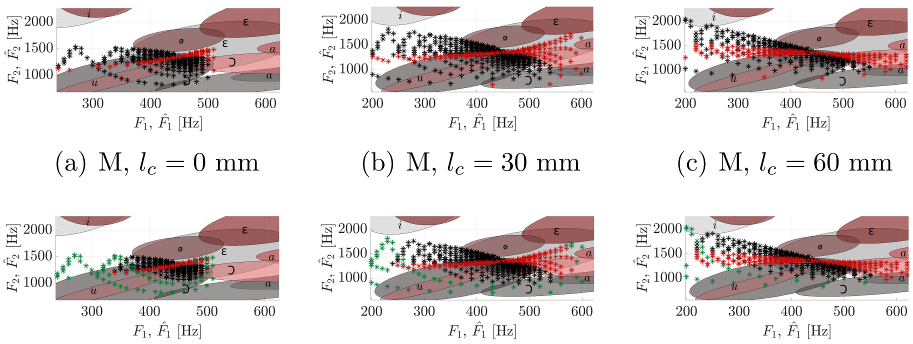

(a) M, $l_c = 0$ mm (b) M, $l_c = 30$ mm (c) M, $l_c = 60$ mm

(d) R, $l_c = 0$ mm (e) R, $l_c = 30$ mm (f) R, $l_c = 60$ mm

Figure 9: Illustration of the limitation of physical constraints on the theoretical resonance space $(\hat{F}_1, \hat{F}_2)$ for one constriction using the SWVT parameter space $(L_0 = 180 \text{ mm}, l_c \in \{0, 30, 60\} \text{ mm}, x_c, \mathcal{P})$ without constraint (theory, black), with restricted x_c-range (R and M, red) and with restricted $\mathcal{P} > 96\%$ (R, green).: a-c) molded waveguides (M); d-f) rigid waveguides (R). Vowel formant spaces (F_1, F_2) are plotted as a reference.

Not all selected SWVT parameter subsets for a given American English vowel, based on the MRI_{II}-criterion (see Fig. 9), are experimentally feasible due to the physical constraints listed in the previous paragraph. In such cases, the SWVT parameters are re-selected using the formant space-based **Peterson**-criterion, following the same way approach applied to French vowels using the **Calliope**-criterion. An overview of the SWVT waveguide parameters used for experimental validation with both rigid (R) and deformable (M) waveguides is provided in the following Table 1.

Vowel	**Material**	N_c	$x_{c,1}, x_{c,2}$ [mm]	$\mathcal{P}_1, \mathcal{P}_2$ [mm]	$l_c^\dagger$ [mm]	Er_{12} [%]
/a_0/	R, M	1	-144, 0	96, 0	0	22
/a_{30}/	R	1	-151, 0	96, 0	30	10
/a_{60}/	R	1	-132, 0	96, 0	60	12
/i_0/	R, M	1	-54, 0	96, 0	0	28
/i_{30}/	R, M	1	-56, 0	96, 0	30	7
/i_{60}/	R, M	1	-56, 0	93, 0	60	2
/u_0/	R, M	1	-93, 0	76, 0	0	42
/u_{30}/‡	R	1	-19, 0	71, 0	30	37.80
/u_{60}/	R, M	1	-90, 0	68, 0	60	42
-	-	-	-	-	-	-
/$i_{1,0}$/	M	1	-51, 0	96, 0	0	38
/$i_{2,0}$/	M	1	-60, 0	96, 0	0	24
/$i_{1,30}$/	M	1	-61, 0	96, 0	30	29
/i_0/	M	2	-50, -70	98, 99	0	8
/u_0/	M	1	-108, 0	96, 0	0	14
/$u_{2,0}$/	M	1	-123, 0	99, 0	0	19
/$u_{3,0}$/	M	1	-134, 0	99, 0	0	21
/u_{30}/	M	1	-89, 0	76, 0	30	41
/$u_{1,30}$ /	M	1	-122, 0	99, 0	30	26
/$u_{2,30}$ /	M	1	-19, 0	96, 0	30	36
/$u_{3,30}$ /	M	1	-19, 0	99, 0	30	36
/u_0/	M	2	-20, -95	98, 99	0	0
/$u_{1,0}$/	M	2	-20, -140	90, 96	0	29
/u_{30}/	M	2	-61, -121	96, 99	30	15

† $l_{c,1} = l_{c,2} = l_c$ for two constrictions ($N_c = 2$).

‡ exit condition not circular, fitted to the waveguide.

Table 1: Experimentally feasible SWVT parameters selected for waveguides representing American English vowels, labeled as /$a_{\cdot,l_c}$/, /$i_{\cdot,l_c}$/, /$u_{\cdot,l_c}$/ with . indexing selections from similar SWVT parameter subsets. The waveguide length is fixed at $L_0 = 180$ mm. The relative difference Er_{12} (in %) is calculated between theoretical resonance frequencies of listed SWVT waveguides and those from MRI_{II}. Highlighted rows (in gray) indicate cases where the **Peterson**-criterion was used because the SWVT parameters based on the $\mathbf{MRI}_{II}$-criterion were not experimentally feasible. $N_c \in \{1, 2\}$ denotes the number of constrictions.

3.2 Experimental validation: Geometry validation for deformable molded waveguides

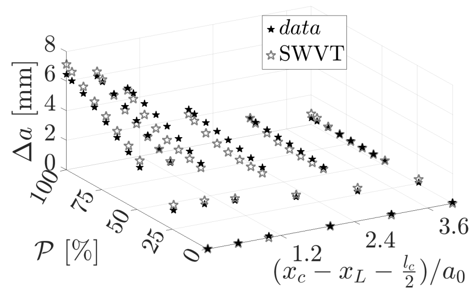

(a) $l_c = 0$ mm

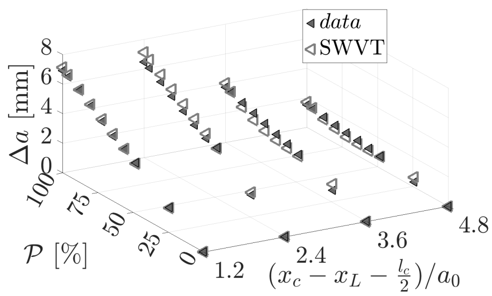

(b) $l_c = 30$ mm

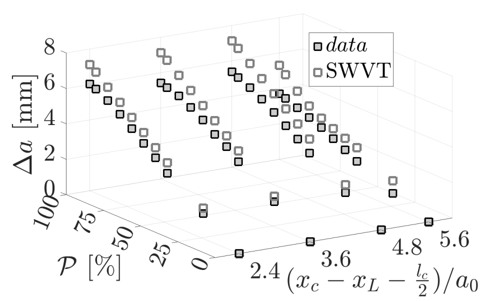

(c) $l_c = 60$ mm

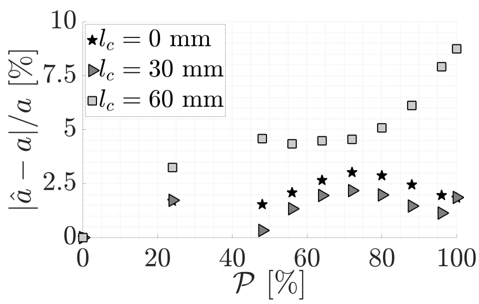

(d)

Figure 10: a-c) Comparison between the measured (data) and theoretical (SWVT) wall displacement Δa (in mm) as a function of constriction degree $\mathcal{P}$ (in %) and normalized position $(x_c - x_L - l_c/2)/a_0$ for $l_c \in \{0, 30, 60\}$ mm; d) mean relative error (in %) as a function of $\mathcal{P}$ (in %) between the measured major axis $a \approx \Delta a + a_0$ and theoretical major axis $\hat{a}$.

3.3 Validation of rigid and deformable SWVT waveguides, /i/, /a/, /u/

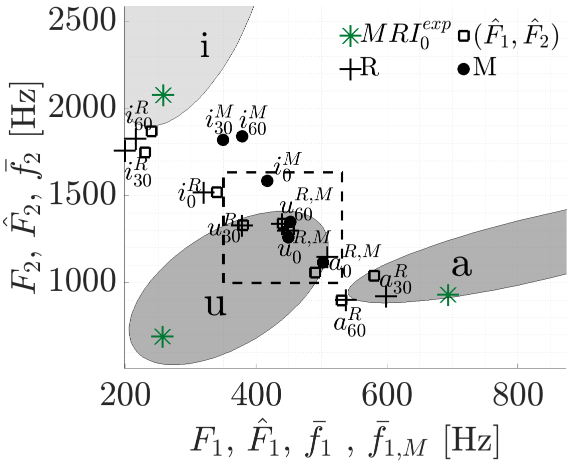

(a) full view

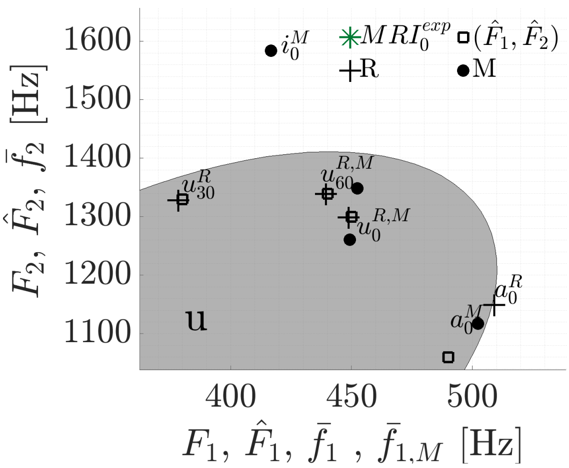

(b) zoomed view

Figure 11: Theoretical $(\hat{F}_1, \hat{F}_2)$ and experimentally measured resonance frequencies $(\overline{f}_{1,M}, \overline{f}_2)$ for deformable (M) SWVT waveguides and $(\overline{f}_1, \overline{f}_2)$ for rigid (R) waveguides (SWVT, MRI_0^{exp}). One constriction cases selected from SWVT subset $(L_0 = 180 \text{ mm}, l_c \in \{0, 30, 60\} \text{ mm}, x_c, \mathcal{P})$, shown both in full view (a) and zoomed view (b). Formant spaces (F_1, F_2) for the American English vowels /i/, /a/, /u/ are shown for reference.

3.4 Overall view of measured resonance frequencies: influence of l_c and S_c

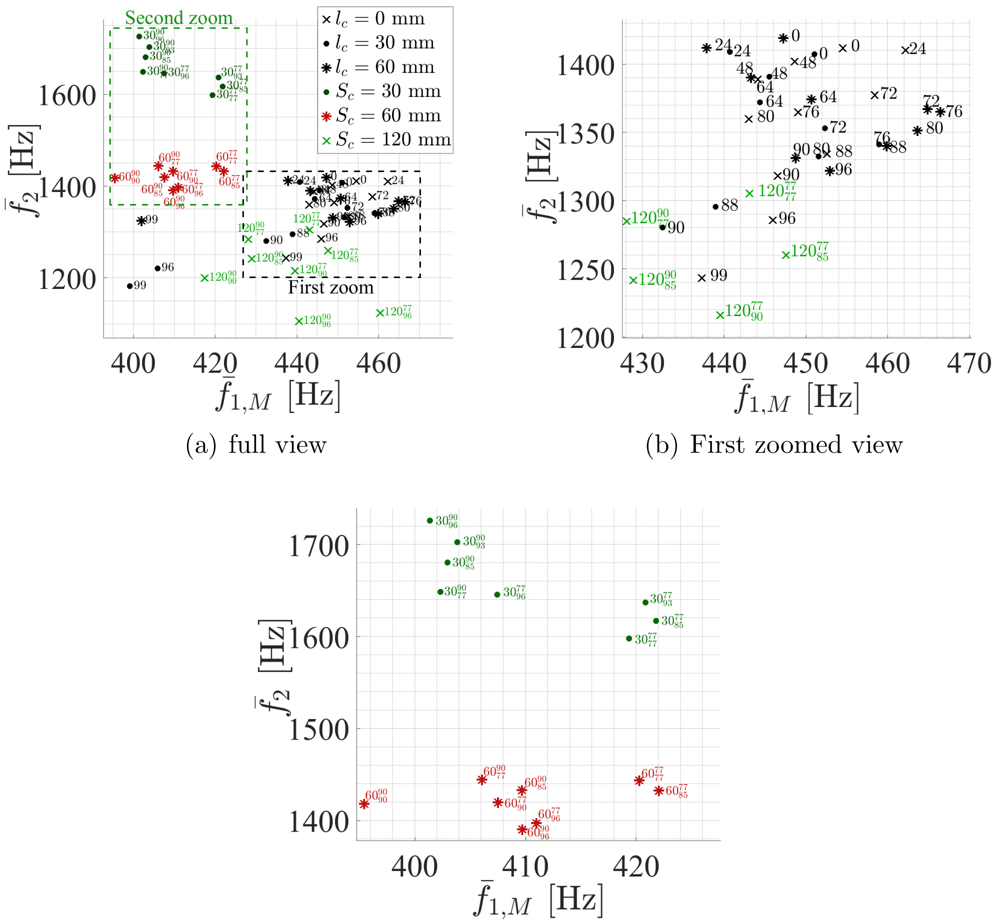

(a) full view

(b) First zoomed view

(c) Second zoomed view

Figure 12: Overview of the measured resonance frequencies ($\overline{f}_{1,M}, \overline{f}_2$) illustrating the influence of the pincher extent length l_c (for one constriction configurations; indicated by black symbols and $\mathcal{P}$) and the constriction spacing S_c (for two constriction configurations with $l_{c,1} = l_{c,2} = 0$ mm; indicated by non-black symbol and $S_{c\mathcal{P}_2}^{\mathcal{P}_1}$): a) overall full view, b) first zoomed view, c) second zoomed view.